frontiers | Frontiers in Earth Science

TYPE Original Research
PUBLISHED 05 January 2023
DOI 10.3389/feart.2022.1030224

OPEN ACCESS

EDITED BY
Zihua Tang,
Institute of Geology and Geophysics (CAS), China

REVIEWED BY
Shixiong Yang,
Qingdao Institute of Marine Geology (QIMG), China
Li Wu,
Anhui Normal University, China

*CORRESPONDENCE
Guangyang Wu,
guangyangwu@henu.edu.cn

SPECIALTY SECTION
This article was submitted to Quaternary Science, Geomorphology and Paleoenvironment, a section of the journal Frontiers in Earth Science

RECEIVED 28 August 2022
ACCEPTED 26 September 2022
PUBLISHED 05 January 2023

CITATION
Pan Y, Mu G, Gao C, Behling H, Liu D and Wu G (2023), Charcoal in Kunlun Mountains loess: Implications for environment change and human activity during the middle Holocene.
Front. Earth Sci. 10:1030224.
doi: 10.3389/feart.2022.1030224

Charcoal in Kunlun Mountains loess: Implications for environment change and human activity during the middle Holocene

Yanfang Pan[1,2], Guijin Mu[3], Cunhai Gao[4], Herman Behling[5], Dexin Liu[1,2] and Guangyang Wu[1,2]*

[1]National Demonstration Center for Environmental and Planning, College of Geography and Environmental Science, Henan University, Kaifeng, China, [2]Key Laboratory of Geospatial Technology for the Middle and Lower Yellow River Regions, Henan University, Ministry of Education, Kaifeng, China, [3]Xinjiang Institute of Ecology and Geography, Chinese Academy of Sciences, Urumqi, Xinjiang, China, [4]Ontario Geological Survey, Sudbury, ON, Canada, [5]Department of Palynology and Climate Dynamics, Albrecht-von-Haller-Institute for Plant Sciences, University of Göttingen, Göttingen, Germany

Loess sediment charcoal records are used in paleoecological analyses to reconstruct fire history and human activities. The Tarim Basin is bordered to the south by the Kunlun Mountains, where eolian silt or loess is extensive and has continued to be deposited in modern times. In this study, we conducted multiple analyses of a 720 cm–thick loess section (KLA) at 3,516 m elevation in the Kunlun Mountains to reconstruct the middle Holocene vegetation history in northern China. Our palynological, charcoal, and grain-size data reveal a slightly drying trend with notable moisture fluctuations in the Kunlun highland since ~4.9 kyr (1 kyr = 1,000 cal yr BP). At approximately 4.1, 2.0, and 1.0 kyr, the climate became more arid; the intervals of 4.0–3.2, 2.4–1.9 and 0.7–0.5 kyr were relatively wet periods. Some sand activity phases in the southern margin of the Taklimakan Desert are recorded around 4.0–3.5, 2.5–2.3, and 1.2–0.7 kyr. Stronger human activities commenced at approximately 2.0 kyr. On the basis of sedimentary charcoal concentrations and regional paleoclimatic and archaeological records, we propose that micro charcoal (<50 μm) originated from the Tarim Basin, reflecting human activity in the basin. Macro charcoal (>50 μm) is suitable for reconstructing Kunlun highland fire events. We suggest that increased anthropogenic activities such as agriculture, construction, and wars played an important role in land degradation and abandonment of ancient cities in the southern Tarim Basin. Our results provide new insights into the role of humans in the ecological evolution of inland arid areas in China during the middle Holocene.

KEYWORDS

middle Holocene, Tarim Basin, loess sediment, charcoal, human activity

1 Introduction

When considering human–land relationships, it is essential to comprehend the interactions between environmental changes and human activities. As a key part of arid central Asia, northwest China has a hyperarid climate and thus a fragile ecology that is extremely sensitive to climatic change. Within this region, the Taklimakan Desert is located in the interior of the Eurasian continent, far from the ocean and surrounded by huge mountains on all sides. The desert is one of the driest and most ecologically sensitive regions in China (Zhu et al., 1981; Domrös and Peng, 1988; Hovermann and Hovermann, 1991; Jakel, 1991; Yang, 1991; Goudie, 2002; Yang et al., 2004). Hundreds of relics spanning the late Paleolithic Age to the historic period have been found within and surrounding the desert, suggesting a long history of human settlement in the region (Li J., 1985; Xi, 1988; Du, 1996). Radiocarbon dating and the stratigraphic relations between stone artifacts and the sedimentary succession indicate that human activity in the area could extend back to approximately 13 kyr. Especially from the Han Dynasty (206 BC–220 AD) to the Tang Dynasty (618–907 AD), the region flourished and was an important part of the southern route of the Silk Road; however, many ancient cities have become isolated ruins (Xi, 1988). There are many different hypotheses for the cause of city abandonment, including climatic aridification (Zhong et al., 2001; Shu et al., 2007), war damage (Li Y 1985), changes to river courses, river shortening (Zhu and Lu, 1991; Chen et al., 2011), and sudden disasters.

The interaction of climate and human activities in the Tarim Basin is a long-standing controversial subject (An et al., 2006; Chen et al., 2006; Huang et al., 2021; Zhou et al., 2021). One of the greatest difficulties in studying dryland degradation and climate change is separating the effect of human activity from the effects of climatic fluctuations (Dodson et al., 2004). Because of the lack of continuous, high-resolution records in the southern Tarim Basin, research on this topic is challenging. Recent studies in this region suggested the prevalence of a dry climate in the early Holocene and relatively wetter conditions in the middle and late Holocene (Zhao et al., 2007; Chen et al., 2008). Additionally, not much is known about human impacts on the vegetation and fire history in this region. To investigate anthropogenic signals, it is necessary to establish a record of human activity derived from proxy indicators. Charcoal, the product of the incomplete combustion of plant material, is embedded in the soil and can be used to reconstruct a chronological sequence of fire frequency over thousands to tens of thousands of years. A higher charcoal concentration generally corresponds to more intense and frequent wildfires. Wildfire activity is related to both climatic changes and human activities (Goldberg, 1985; Clark, 1988; Hui et al., 2021).

In this study, a 720 cm–thick loess section (KLA) at 3,516 m above sea level (asl) in Kunlun Shan (Mountains) was studied on the basis of multiple proxies (Figure 1). Charcoal, palynological, and grain-size data were used to reconstruct past climate changes and further explore the evolution of fire in the southern Tarim Basin, allowing discussion of the interactions of wildfire, climatic changes, and human activities.

2 Physical geography of the study area

The study area is located in the headwaters of the Nu'er River in the middle Kunlun Mountains. The mountain range has an average elevation of 5,500 m asl with many peaks standing above 6,000 m asl. Along the northern slope of the Kunlun Mountains, there are extensive loess deposits on varying geomorphic surfaces (e.g., terraces and foothills) between 2,000 and 4,500 m asl (Fang et al., 2002). Because of the southward bending of the eastward-aligned Kunlun Mountains, low-level meridional air flows over the Tarim Basin converge at the apex from Hetian to Yutian, resulting in frequent dust storms and accumulation of airborne fine particles up to 200 m thick on the mountains in this area (Figure 1) (Han et al., 2006; Liu et al., 2010; Zan et al., 2010; Chen et al., 2022). This process commenced probably a million years ago, and continued throughout the Holocene to the present day (Gao, 2004; Yang et al., 2021). The middle Kunlun Mountains loess is light yellowish-gray in color, and contains no obvious carbonate nodules or paleosol horizons. The loess deposit consists of loosely packed silt to very fine sand particles with finer material filling the voids. The pH values are 7.5–9.2, and illite is the predominant clay mineral (<0.002 mm) (Gao and Zhang, 1991; Zhao et al., 1995).

Annual precipitation is less than 50 mm at the southern rim of the Tarim Basin. In this area, there are more than 200 days annually with dust concentrations so dense that the visibility is markedly reduced, particularly between Hetian and Yutian (Liu et al., 2010). The annual precipitation increases to approximately 400 mm on the mountains at 4,000 m asl, but the climate is still too dry for regional forest to develop in the middle Kunlun Mountains; instead, alpine steppe and semi-steppe grow at 3,000–4,200 m asl. In the basin, the vegetation is sparse, and Gobi Desert and drift sand dunes are extensive (Cui et al., 1988). Alpine meadows are developed in shady areas at 3,800–4,200 m asl and alpine deserts above 4,200 m asl. The distribution of alpine loess approximately follows the boundaries of the alpine steppe and semi-steppe (Gao and Zhang, 1991; Li et al., 1993). Loess-like silty sand occurs in areas at lower elevations from 2000 to 2,800 m asl. These sediments consist of up to 90% fine to very fine sand, probably resulting from near-surface sand storms in the Tarim Basin (Zhao et al., 1995; Yang et al., 2002).

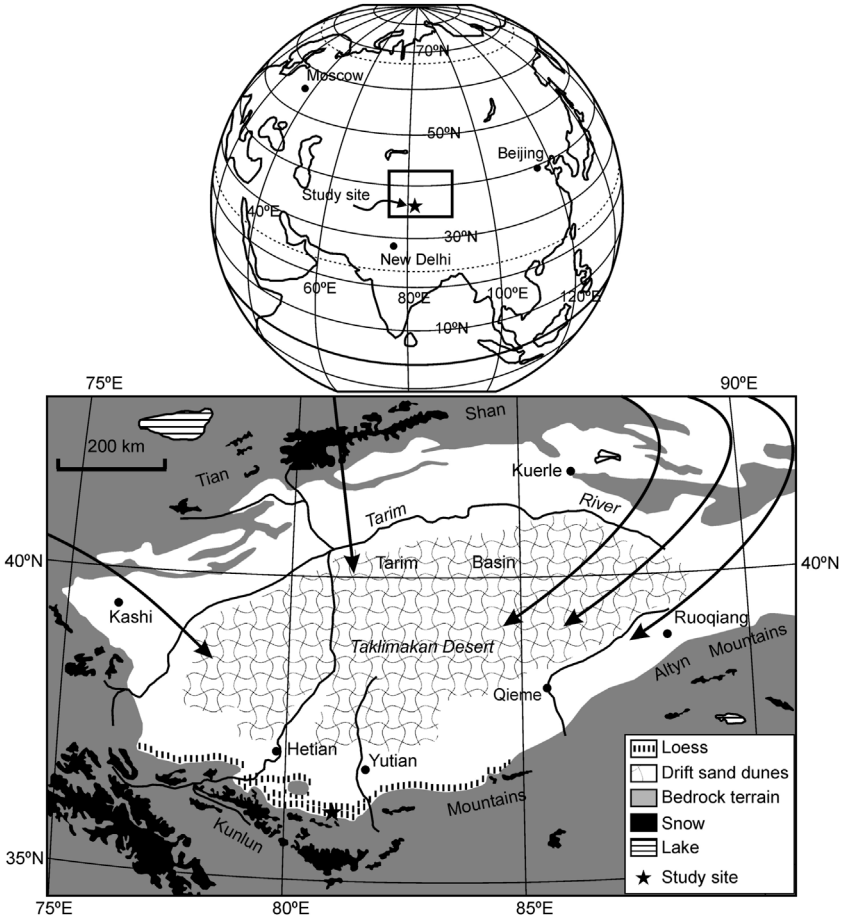

FIGURE 1
Location map showing the study site, regional physiography and the major loess deposit on the Kunlun Mountains. Data sources: Gao and Zhang (1991), Li et al. (1993) and Sun (2002) for loess; and Han et al. (2006) for prevailing winds.

3 Material and methods

3.1 Loess section

The 720 cm–thick loess section (KLA), located at 3,516 m asl (36°03.534′N, 81°04.373′E), was sampled at 2 cm intervals from its base on an older moraine approximately 400 m north of a modern glacier that extends down to 4,100 m asl. The loess is silt-textured and calcareous and shows no visible hiatus. This section is typical for this area and loess with comparable thickness is common on such moraines at 3,500 to 3,800 asl. Analyses of charcoal, pollen and grain size were subsequently undertaken. Four samples were collected from the sediments for accelerator mass spectrometry (AMS) ^{14}C dating. As discussed above, accumulation of such a thick, evenly textured loess deposit implies the presence of a persistent and relatively steady atmospheric circulation responsible for entraining and transporting dust particles to such a high altitude. Because dust storms occur mostly in May to August (Liu et al., 2010), changes in the grain size of the loess reflect the variability in summer wind stress in this region; therefore, detailed grain-size analysis is imperative for a better understanding of the past atmospheric circulation conditions in this region.

3.2 Age control

For age control, samples were collected at horizons containing organic seams and streaks, and plant fragments were picked out for AMS radiocarbon dating. These organic seams formed by *in situ* accumulation of plant litter and were contemporaneous with dust precipitation. Charcoal-like plant fragments from depths of 188, 480, 598, and 670 cm were picked under a binocular microscope from the >0.125 mm residue derived from 100 g of loess material after washing. Each sample weighed between less than 1 and slightly more than

TABLE 1 AMS^{14}C dates for KLA loess section.

Lab #	Sample #	Depth (cm)	Material	^{14}C age (year BP)	Calibrated^{14}C age (2σ, cal year BP)
A1624	Pan 532	188	Plant macrofossils	1,290 ± 15	1,282–1,175
A1624	Pan 240	480	Plant macrofossils	3,055 ± 15	3,348–3,211
A1624	Pan 122	598	Plant macrofossils	3,680 ± 15	4,088–3,932
A1624	Pan 50	670	Plant macrofossils	4,110 ± 15	4,801–4,529

2 mg. In previous studies, large bulk samples were washed to extract sufficient organic material for conventional radiocarbon dating (Gao and Zhang, 1991; Li et al., 1993; Zhao et al., 1995; Tang et al., 2009); however, such samples may incorporate modern plant roots or old plant debris of unknown source that fell out together with lithogenic particles in airborne dust.

3.3 Charcoal and pollen analysis

For the extraction of pollen and charcoal, 74 subsamples, each with a volume of 2 cm^3, were taken from the section at 10 cm intervals from the surface (0 cm) to the bottom (720 cm). Processing was carried out using standard pollen analytical methods, modified from Fægri and Iversen (1989). One tablet of *Lycopodium clavatum*, containing 20,848 ± 1,546 spores, was added to each subsample to enable calculation of pollen and charcoal concentrations. For charcoal analysis, a traverse of the middle of the slide was made and charcoal particles were counted to a total of 100 *L. clavatum* spores to ensure a charcoal concentration estimate with an error of less than 5% (Finsinger et al., 2008). The counted charcoal particles were classified into four groups of different particle sizes to provide more detailed evidence of fire history in terms of distances of fires from the study site. The particle size groups were 10–25, 25–50, 50–100 and >100 μm. For size measurements, the longest axis of each charcoal particle was measured (Whitlock and Larsen, 2001; Sadori and Giardini, 2007).

4 Results

4.1 Chronology

Four radiocarbon dates were used to create a chronology for the KLA loess section (Table 1). Samples were AMS radiocarbon dated at the Radiocarbon Dating Laboratory, the Illinois State Geological Survey, United States, and yielded uncalibrated ages of 1,290 ± 15, 3,055 ± 15, 3,680 ± 15, and 4,110 ± 15 ^{14}C year BP (defined as before 1950). All radiocarbon dates were calibrated using OxCal4.4 (Ramsey, 2008; Ramsey and Lee, 2013) with the IntCal20 calibration dataset (Reimer et al., 2020). Assuming a constant or quasi-constant accumulation rate for the loess, the lower contact of the loess section was estimated to be dated to 4,944 cal year BP (Figure 2). This estimate is consistent with the ages in a neighboring section located at 3,750 m asl (36°3′20.3″ N, 81°2′51.2″ E), for which Gao and Zhang (1991) dated a bulk sample containing streaks of plant debris at 400–500 cm depth and obtained an age of 4,450 cal year BP (5,338 ± 132 ^{14}C yr BP), overall matching the trend of the current radiocarbon dates. The "CLAM" program (Blaauw, 2010), implemented with "R" software, was used to establish an age–depth model (Figure 2) (R Development Core Team, 2010).

4.2 Charcoal record

A total of 74 samples of charcoal from the KLA section were analyzed, with a resolution of approximately 67 years, and four groups of particle sizes were identified. Through the section, the concentration of charcoal particles >100 μm was very low, accounting for 1%–3% of the total (Figure 3). This paucity of larger particles may have been caused by filtering and crushing of large particles during pretreatment (sieving and centrifugation). However, we prepared each sample following the method of Stevenson and Haberle (2005) and adapted from Rhodes (1998), and thus consider that charcoal particles >150 μm were sparse; therefore, we focused on charcoal particles <100 μm. On the basis of visual inspection of the charcoal and pollen assemblages, as well as cluster analysis, the section was divided into five zones (Figure 3).

4.2.1 Zone 1 (720–598 cm, 4.9–3.9 kyr)

Zone 1, at the bottom of the section, is characterized by marked fluctuations in charcoal concentration. Several charcoal peaks were identified in this zone. The average concentration of charcoal particles <50 μm was 46 × 10^3 particles/cm^3, and that of particles >50 μm was 3.9 × 10^3 particles/cm^3. The concentration of charcoal particles >100 μm was very low, only 0.59 × 10^3 particles/cm^3. The concentration of micro charcoal (<50 μm) exhibited fewer fluctuations in the lower part of the unit.

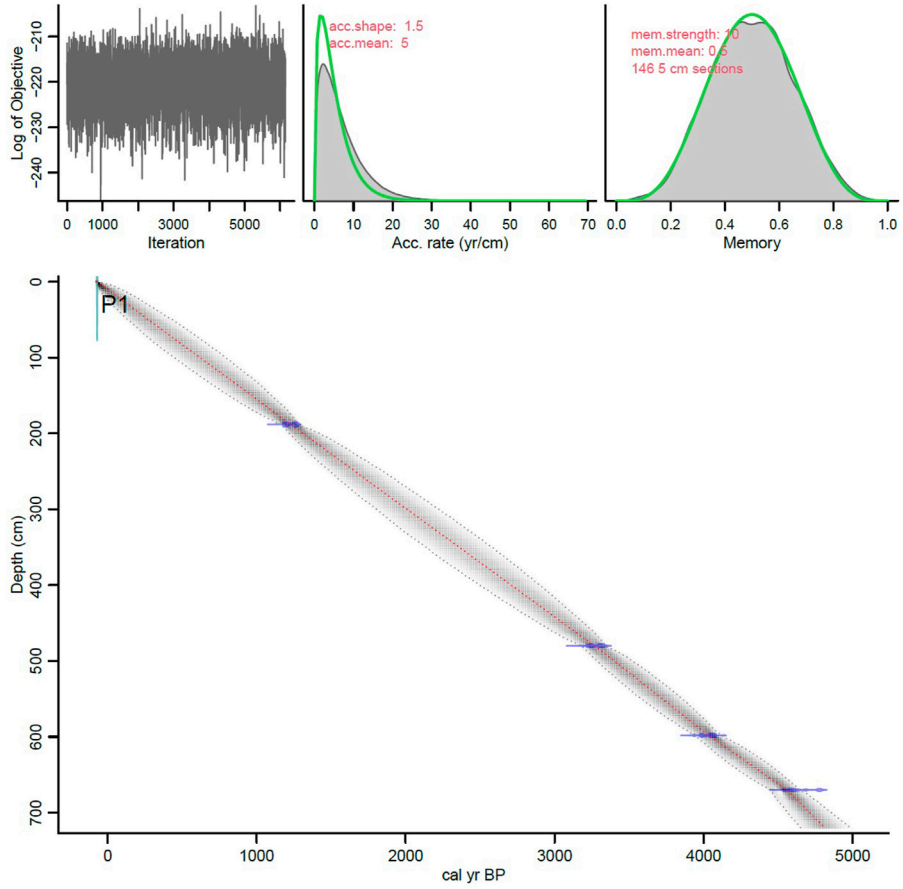

FIGURE 2
Age-depth model for the loess deposit of KLA section.

4.2.2 Zone 2 (598–410 cm, 3.9–2.7 kyr)

The second highest microscopic charcoal concentration was found at 3.2 kyr (83 × 10^3 particles/cm^3), and this peak was followed by a sharp downturn in the composite record. The peak was coincident with a black line at 485–465 cm depth that was observed during field sampling. During 3.9–3.2 kyr, the concentrations of charcoal particles both <50 μm and >50 μm (41 × 10^3 and 3.4 × 10^3 particles/cm^3, respectively) fluctuated but tended to be stable. During 3.2–2.7 kyr, that concentration of charcoal particles <50 μm fluctuated less and stabilized, but that of particles >50 μm fluctuated greatly.

4.2.3 Zone 3 (410–380 cm, 2.7–2.5 kyr)

The most significant characteristic of this zone is that the charcoal particles 50–100 μm with a minimum concentration of 1.7 × 10^3 particles/cm^3, total charcoal concentrations vary between 41.5 × 10^3 and 48.8 × 10^3 particles/cm^3. The average concentration of charcoal particles <50 μm was 43 × 10^3 particles/cm^3, and that of particles >50 μm was 2.7 × 10^3 particles/cm^3.

4.2.4 Zone 4 (380–120 cm, 2.5–0.7 kyr)

Zone 4 is characterized by mostly very high charcoal concentrations of up to 82 × 10^3 particles/cm^3. The charcoal concentration fluctuated greatly during this zone, which displayed the most obvious variations in charcoal concentration of the whole section, with several peaks. The average concentrations of each particle size class showed obvious peaks during this period, with frequent fluctuations. Charcoal particles <50 μm and >50 μm both exhibited maximum values at ca. 1.2 kyr. Charcoal <50 μm occupied a large proportion of the total charcoal, and the average concentration of particles >50 μm was lower. In this zone the five highest charcoal peaks occurred (>70 × 10^3 particles/cm^3 in each peak).

4.2.5 Zone 5 (188–0 cm, 0.7–0 kyr)

A maximum, corresponding to the highest charcoal concentration in the past 4,900 years, occurred around 1880 AD (125 × 10^3 particles/cm^3). This maximum was followed by a sharp decline. From 0.7 kyr until 1880, there

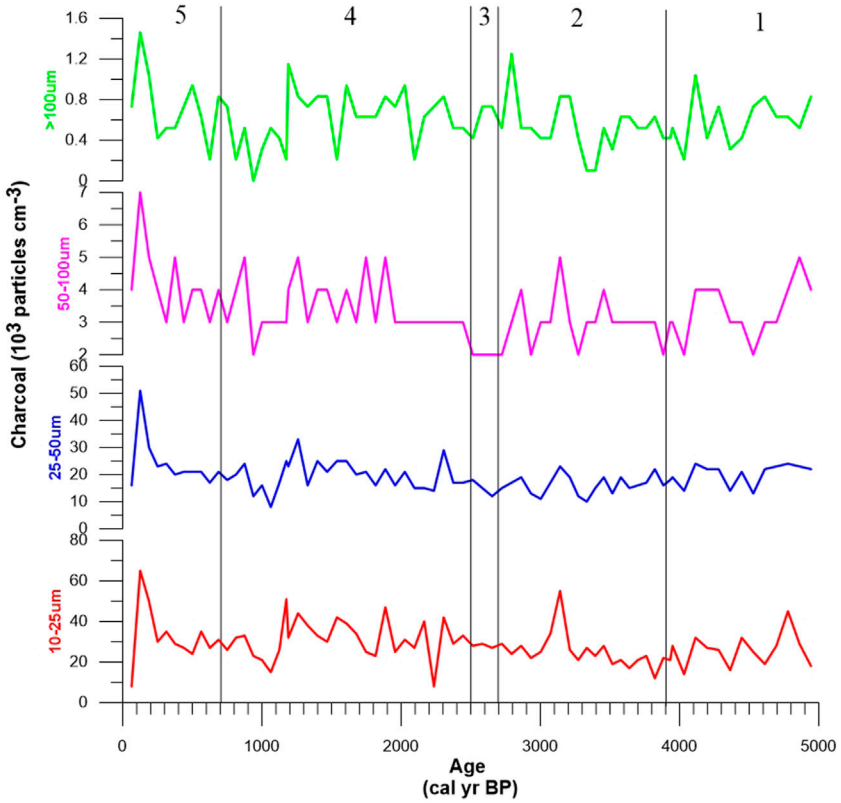

FIGURE 3
Diagrams showing charcoal concentrations in the KLA section.

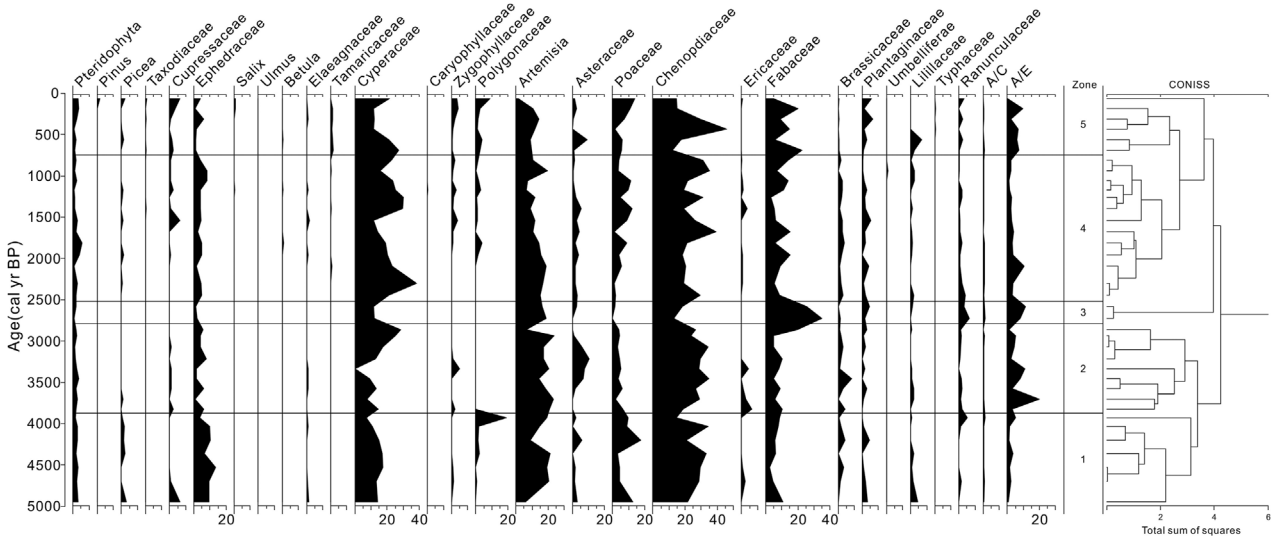

FIGURE 4
Pollen percentage diagram for KLA section.

appears to have been a long-term decline in biomass burning in the southern Tarim Basin.

4.3 Pollen assemblages

The pollen from the loess samples is dominated by Cyperaceae (0%–39.29%), Chenopodiaceae (13.12%–48.77%), *Artemisia* (1.57%–27.59%), and *Ephedra* (1.11%–13.44%), followed by Poaceae (0%–13.39%) and Asteraceae (0%–9.71%), broadly matching the pollen assemblage in the surface samples. Pollen from the deciduous trees *Betula*, *Ulmus* and *Salix* together can reach 2% in some samples; these pollen grains likely originated from woodlands in the nearby river valleys. Pine and Spruce pollen formed less than 3% of the assemblage, suggesting distant sources for these taxa. The pollen concentration varied from 2.25 to 21.34 × 10^3 grains/cm^3, with the maximum at ca. 2.8 kyr rather than at the surface (Figure 4). This result suggests an insignificant role of post-depositional oxidation in pollen preservation in the loess at this site. Assuming a constant sedimentary rate for the loess, the change in pollen concentration is likely related to the density of the regional vegetation cover.

There is a clear trend up the section of a decline of *Ephedra* and *Artemisia* and a gradual increase of Poaceae and Cyperaceae, although the percentage of Chenopodiaceae remained largely unchanged. Five pollen zones can be defined on the basis of the fluctuations in the abundances of these taxa. Zone 1 (4.9–3.9 kyr) has the highest frequency of *Ephedra* and high Poaceae and Cyperaceae. Zone 2 (3.9–2.7 kyr) exhibit low pollen concentrations with elevated levels of Cyperaceae, although Chenopodiaceae remains high in frequency throughout. This zone contain the highest abundances of *Artemisia* and the highest pollen concentration (2.24–9.98 × 10^3 grains/cm^3). Zone 3 (2.7–2.5 kyr) the ratio of *Artemisia* to Chenopodiaceae (A/C) and the ratio of *Artemisia* to *Ephedra* (A/E) were highest in these zones. In contrast to the previous zones, Zone 4 (2.5–0.7 kyr) exhibited a marked reduction in *Ephedra* and expansion of Poaceae and Cyperaceae, with a pollen concentration up to 17.85 × 10^3 grains/cm^3. In the succeeding Zone 5 (0.7 kyr to the present day), *Ephedra* remained low and Poaceae and Fabaceae exhibited relatively high percentages throughout, with a maximum pollen concentration of 17.27 × 10^3 grains/cm^3.

5 Interpretation and discussion

5.1 Middle Holocene vegetation and climate dynamics

The multi-decade-resolution record of climate, pollen (A/C and A/E ratios) and grain size in the KLA section reveals a slightly drying trend with marked moisture fluctuations and intensifications in atmospheric circulation in the southern margin of the Tarim Basin since ~4.9 kyr (Figures 5, 6).

In general, pollen assemblages reflect the regional vegetation. Although extremely sparse plants occur in the hyperarid Tarim Basin, the pollen deposited in the KLA section mainly reflects the vegetation on the highlands, which are dominated by local moisture. In the study region, precipitation and moisture in the growing season is the predominant limiting factor for vegetation. Although shrubs such as *Ephedra* can grow under dry, desert conditions, grass cannot survive severe summer droughts. The A/C ratio has been widely used as an index for desert and steppe: higher values indicate a larger steppe (El-Moslimany, 1990; Chen et al., 2006; Zhao et al., 2007; Tang et al., 2009, Tang et al., 2013). Chenopodiaceae, although they are adapted to desert conditions, are not uncommon in other ecological zones, but *Ephedra* is confined mainly to deserts. The A/E ratio is also a useful index of moisture conditions. Although the ratio is useful in data interpretation where pollen assemblages consist predominantly of these two plants, use of this index should be site-specific, in particular, where the pollen assemblage contains high percentages of *Ephedra*, as in this study (Cour et al., 1999; Luo et al., 2009). Thus, the fluctuations of *Artemisia* and *Ephedra* in the pollen record indicate that the climate became progressively drier during summer over the last 4,900 years (Figures 5B,C). The decrease in moisture over the last two millennia appears to be consistent with the nearby Guliya ice core record that exhibits a slight rise in temperature in the late Holocene (Figure 6B) (Yao et al., 1996; Thompson et al., 1997).

Grain size is a proxy for wind stress related to the lower atmospheric circulation over the Tarim Basin. The grain-size analysis demonstrated that the samples have a median grain size (Mz) of 40.47 μm (36.17–50.32 μm) and contain predominantly silt (2–63 μm, 63%–73%) and very fine sand (63–125 μm, 25%–34%) with limited fine sand (125–250 μm, 3%–8%) and clay (<2 μm, 3%–5%). The grain-size distribution is comparable with that of a modern dust sample collected from the KLA site at approximately 3,516 m asl. This finding is consistent with the observed dusty weather from early March to mid-May every year on the northern slope of the Kunlun Mountains. In contrast to the Loess Plateau in central China, where the sand fraction is generally less than 20% (Liu, 1965), the loess in the study area is coarser because of its proximity to the source area in the Tarim Basin to the north.

We used the grain-size content (p > 63 μm) to reflect the advance and retreat of the Taklimakan Desert and wind intensity (Tang et al., 2009, 2013). Through the section, the grain-size curve shows intervals of coarser material at 4.0–3.3 and 1.2–0.7 kyr (Figures 5A, 6E). The grain size does not respond to changes in humidity or vegetation under arid and superarid

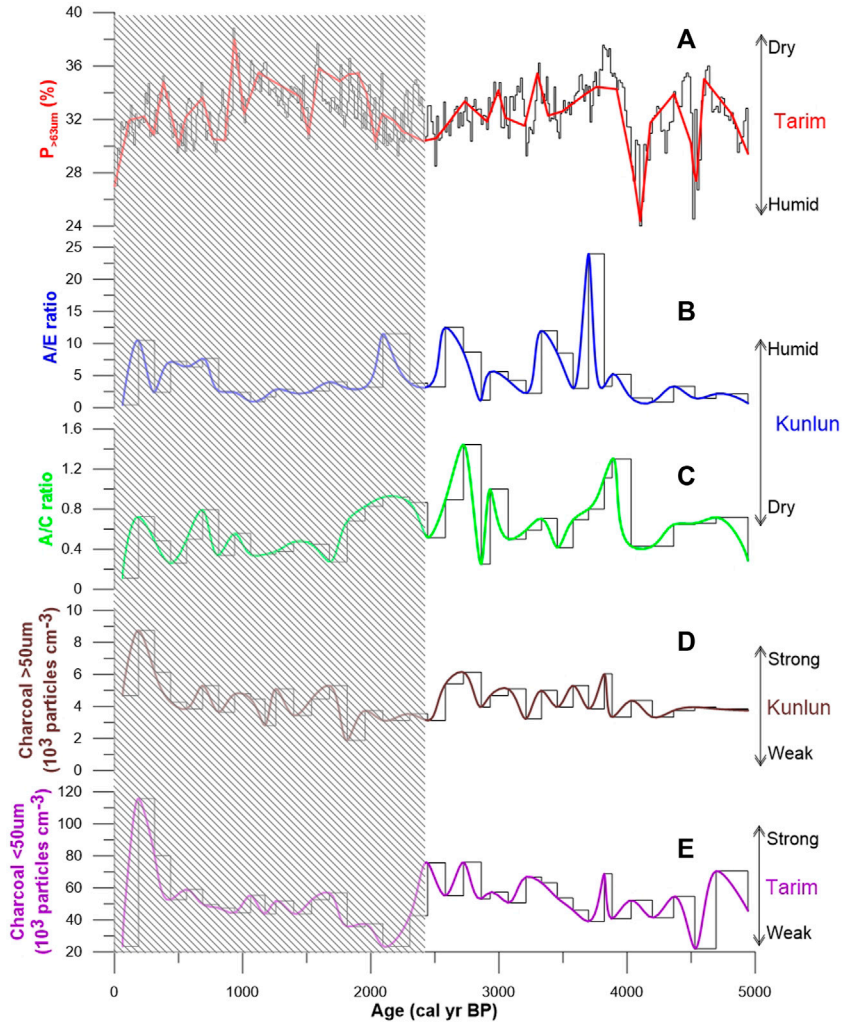

FIGURE 5
Variations of the proxies for KLA section: **(A)** p > 63 μm sand content; **(B)** the ratio of Artemisia to Ephedra (A/E); **(C)** The ratio of Artemisia to Chenopodiaceae (A/C); **(D)** Macro charcoal (>50 μm); **(E)** Micro charcoal (<50 μm). Black shading represents historical period.

conditions. The middle Holocene loess in the study area is notably less variable in grain size than older loess deposits that accumulated over the last million years, suggesting that the source area and atmospheric circulation were relatively stable during the middle Holocene (Fang et al., 2002; Zan et al., 2010; Zheng et al., 2022). However, the grain-size curve in the loess section suggests intensification in atmospheric circulation during the last 2,000 years. Dust precipitation in the Tarim Basin occurs mostly in the summer when the lower atmospheric circulation is dynamic, and is minimal during the winter when near-surface air convection remains less active (Liu et al., 2010). Assuming that this pattern was the general condition of the entire middle Holocene, the windy episodes recorded in the section were related to periods of increased near-surface convection and enhanced dynamics in atmospheric circulation.

5.2 Origin of paleofire

Fire is a unique and important ecological factor, both in the past and at the present day, and has a marked impact on the environment. Charcoal is the direct product of fire and vegetation and is related to both climatic changes and human activities (Scott et al., 2000; Huang et al., 2006; Tan et al., 2011); therefore, charcoal can be used both to reconstruct ancient fire events and to indicate the strength of human activities. However, there is a serious lack of knowledge about fire's fundamental role in arid regions, as well as an insufficient appreciation of fire's interaction with anthropogenic environmental change (Jiao et al., 2009).

According to the Patterson et al. (1987) model, "large" fragments of charcoal remain closer to the source than do

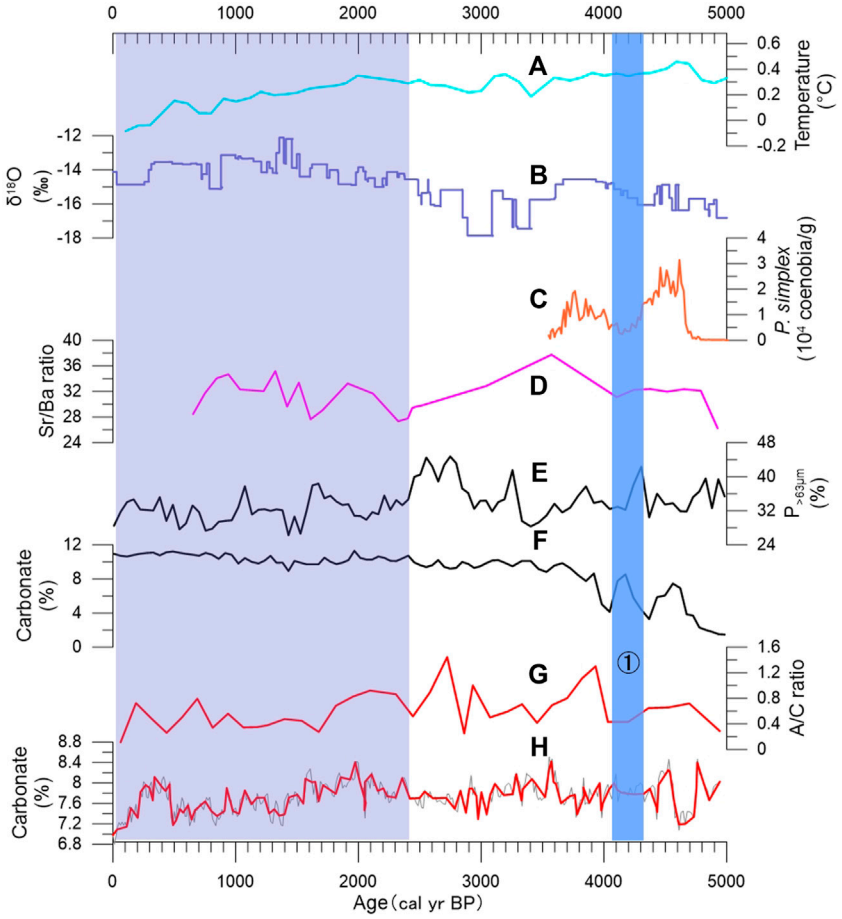

FIGURE 6
Comparison of climatic records of the surrounding area and KLA loess data. **(A)** Mean annual temperature reconstruction for North America and Europe (Marsicek et al., 2018). **(B)** $\delta^{18}O$ record from the Guliya ice core (Thompson et al., 1997). **(C)** Concentration of *P.simplex* in Bosten Lake (Huang et al., 2021). **(D)** Sr/Ba record of Yotgan profile (Zhong et al., 2007). **(E)** p > 63 μm sand content of the Liushui cemetery (Tang et al., 2009). **(F)** Carbonate content of the Liushui cemetery. **(G)** The ratio of Artemisia to Chenopodiaceae (A/C). **(H)** Carbonate content of KLA section. ① Indicate cold events at 4.2–4.1 kyr, respectively. Blue shading represents historical period.

"small" fragments, which are spread evenly over a wider area. Source areas for pollen-slide charcoal are subcontinental to global, and diagrams of pollen-slide charcoal are biased toward nonlocal charcoal. Thus, pollen-slide charcoal can be used to interpret the importance of fire over broad spatial and temporal scales. The presence of high concentrations of charcoal (between 26 and 125 × 10^3 particles/cm^3) in the KLA section implies a prominent role of fire in the Kunlun highlands and Tarim Basin during the middle Holocene. These fires might have been anthropogenic or natural, but, for two reasons, a natural origin of fire is less likely. First, we used the method of Stevenson and Haberle. (2005) to extract large particles (>125 μm), which indicate changes in local wildfire occurrence (Whitlock and Larsen, 2001); there were few of these particles in the KLA section. Second, the lack of simultaneity of the concentration of charcoal particles with climatic change supports the anthropogenic origin of fire. For example, the concentration of charcoal was higher during the 3.7–3.2 and 2.7–2.4 kyr wet periods, but for the periods 3.2–2.7 and 1.9–1.4 kyr, when the area experienced a longer dry season, charcoal concentrations were low (Figures 5D,E, 6D).

Micro charcoal (<50 μm) is thought to be derived primarily from within 20–100 km of the depositional site (Clark and Patterson, 1997). Concentrations of micro charcoal vary between 24 × 10^3 and 116 × 10^3 particles/cm^3 in the KLA section, which may indicate that regional fires occurred frequently during the middle Holocene (Figure 5D). The small charcoal component may have been deposited from atmospheric fall-out together with eolian dust sourced from the Tarim Basin, because both types of particles are easily transported over long distances by wind in dry environments. As discussed above, accumulation of such a thick, evenly textured loess deposit

suggests the presence of a persistent and relatively steady atmospheric circulation responsible for entraining and transporting dust particles to such a high altitude. Because dust storms occur mostly in May to August, changes in the micro charcoal content and grain size of the loess may reflect variability in the summer wind stress in this region. The loess of the Kunlun Mountains is thought to be of eolian origin, because of the relatively short transport distance from the source area in the Tarim Basin (Gao and Zhang, 1995). We infer that the micro charcoal was produced by fires in the Tarim Basin and deposited on the northern slope of the Kunlun Mountains, and thus reflects human activity in the Tarim Basin.

Analyses of the particle-size distributions of macro charcoal (>50 μm) showed that such particles are usually not transported far from fires, and are likely suitable for reconstructing local fire events (mostly within a few hundred meters) (Patterson et al., 1987; Clark, 1988). Concentrations of large-sized charcoal vary between 2.08×10^3 and 8.76×10^3 particles/cm^3 in the KLA section, indicating that fire events occurred locally (Figure 5E). In contrast to micro charcoal, low concentrations of macro charcoal accumulated during the middle Holocene. This finding suggests that local biomass burning was low during the last 4,900 years. However, the charcoal record and history of human activities imply that human-set fires were more common than natural fires during the middle Holocene (Figure 6) (Zu et al., 2003; Xinjiang Archaeological Team, IA, CASS, 2016; Wagner et al., 2011).

In general, peaks of micro and macro charcoal showed different temporal patterns during the middle Holocene interval in the KLA section. The differences in the timing of the trends are not easily explained, and may be caused by real differences in fire history across spatial scales, or may reflect differences in transportation mechanisms (Thevenon et al., 2010). Previous paleoclimatic reconstructions showed anti-phased moisture changes between the southern Tarim Basin and the Kunlun highland during the past 5,000 years, with a nearly seesaw relation between the two areas (Tang et al., 2013). Several aspects of the record can be interpreted in the context of data on climate changes and human activities. In our study, pollen assemblages, A/C ratios and A/E ratios suggest that during the past 4,900 years on the Kunlun highland, the intervals of 4.0–3.2, 2.6–1.9, and 0.7–0.5 kyr were moister and those at 4.9–4.0, 3.2–2.9, and 1.9–1.1 kyr were drier, and the climate and environment became relatively worse (Figure 6). However, the record of $p > 63$ μm fraction from the same samples suggests a different setting. Some sand activity phases in the southern margin of the Taklimakan Desert are recorded at around 4.0–3.2, 2.7–2.4 and 1.9–1.1 kyr, reflecting increased aridity in that area. The most pronounced increases in aridity occurred at approximately 4.0, 2.5, 1.7, 1.0, and 0.5 kyr, indicated by the greater $p > 63$ μm values (Figures 5A,B,D,E).

In the KLA section, at ca. 4.0 kyr, the pollen, grain size, and charcoal abruptly changed, suggesting an alteration in the climate related to short-term climatic events. Many lines of evidence from climatic proxies for the Xinjiang region and other parts of the world have identified a prominent climatic event between 4.2 and 4.0 kyr (Huang et al., 2015; Rao et al., 2019; Huang et al., 2020) (Figure 6). This event was associated with great droughts because of reduced rainfall and river discharges. However, based on *Pediastrum* assemblages and clumped oxygen isotope values of carbonates from Bosten Lake, Huang et al. (2021) recently reported a very warm and humid climate during 4.8–3.6 kyr that was interrupted by a cold event at 4.2–4.0 kyr (Figure 6C). In the present study, the lowest levels of macro and micro charcoal occurred at ~4.0 kyr in the KLA section. Comparing the pollen and charcoal records with archaeological and historical data, we suggest that, because the change in the climate of southern Xinjiang affected the environment (and thus human survival) to a great degree, there was a population decrease at around 4.1 kyr in both the Kunlun highland and the Tarim Basin.

The second highest sedimentary micro charcoal content occurred during 3.3–3.1 kyr in the KLA section (Figure 3). In the Yuetgan profile, Zhong et al. (2007) found that larger particles of charcoal appeared at approximately 3.4 kyr, and related this appearance to sudden drying of the climate (Figures 6D, 7). However, in the KLA section we found that the contents of Cyperaceae and *Artemisia* were relatively high at that time, the pollen concentration did not decrease markedly, and the A/C and A/E values were also stable. And the concentrations of *P. simplex* in Bosten Lake did decrease at the same time, which indicated cold events at 3.6–3.5 kyr (Figure 6C). Therefore, abrupt climate change cannot explain the peak of charcoal at that time. Archaeological evidence indicates that the primitive settlements in this area had entered the Bronze Age at that time. Metallurgical technology improved, with important advances in bronze, gold and iron wares. Metal ornaments, not just production equipment, from this time have been found in the Niya site, Zaghunluq cemetery and Yianbulake site. We suggest that metallurgical technology, in particular the earliest use of iron tools in the Xinjiang region, may be responsible for the highest charcoal levels occurring at 3.3–3.1 kyr.

5.3 Spatiotemporal distribution of ancient relics in the southern margin of the Tarim Basin during the late Holocene

To better understand the impact of the population on the regional environment, we plotted the distribution of ancient relics (based on archaeological documents and historical records) at the southern Tarim basin and the location of other sites referenced in the text during the late Holocene (Figure 7) (Huang, 1981; Li J., 1985). We found the distribution of ancient cities exhibited migration along the middle and lower reaches to the middle and upper reaches of the river through time. Human activities gradually retreated to

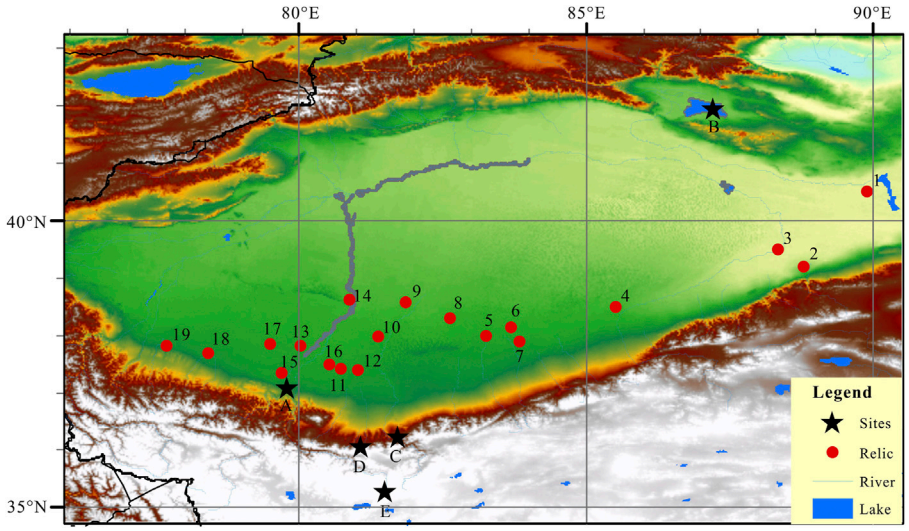

FIGURE 7
Distribution of ancient relics at the southern Tarim basin and the location of other sites referenced in the text. The numbers represent major ancient cities: 1) Loulan, 2) Miran, 3) Luobuzhuang, 4) Qiemo, 5) Andir, 6) Tiran, 7) Dawuzlek, 8) Niya, 9) Kelaton, 10) Dandanwulik, 11) Wucentoti, 12) Laoda mogou, 13) Akspir, 14) Mazarta, 15) Yuetgan, 16) Lafak, 17) Canggui, 18) Pishan, 19) Kehan. The letters represent KLA section and other sites: A Yuetgan, B Bosten Lake, C Liushui, D KLA section, E Guliya.

the piedmont area, and human living spaces dwindled (Zhong and Xiong, 1999). For the ancient cities with definite information on their destruction and abandonment, abandonment times were concentrated in the fourth to fifth, seventh to eighth, and eleventh centuries (Common Era), which may indicate that a variety of sites were abandoned for similar reasons during those times (Shu et al., 2003; Shu et al., 2007). The careful analysis of charcoal particles in the present work provides another method that may give insights about the driving force of the temporal and spatial evolution of ancient cities in the Tarim Basin.

During 2.0–1.2 kyr, charcoal abundance increased notably, whereas the A/C and A/E ratios decreased, the Poaceae and Fabaceae pollen percentages increased, and herb pollen, dominated by Chenopodiaceae and Ephedraceae, was less abundant (Figures 3, 5B,C). The increasing trend of grain size (p > 63 μm) in the KLA section suggest that periods with slightly stronger aridity in the southern margin of the desert coincided with decreased moisture at the KLA section (Figure 5A). The intensity of human disturbance by fire and cultivation appears to have increased during the last 2,000 years. The more pronounced increase in charcoal during 2.0–1.8 kyr can be attributed to the increased human population and the development of agriculture. According to historical records (Liu, 1988), the highest population in the east Han Dynasty was 90,000 in the Hotan region. Subsequently, during the first and second centuries, eight wars broke out between Hotan state and Shache-Hami state, and only approximately 1,000 remained of the 7,000 Hami people; the abundance of micro charcoal was low at this time.

The population of the Tarim Basin decreased during the fourth to sixth centuries: at this time there was a brief low of micro charcoal, indicating a decrease in fire activity. This low also corresponds to the documentary record, which states that during 440–443 AD a war in Yutian killed more than 50% of the region's 80,000 population (Li Y, 1985). At that time, the pollen A/C and A/E ratios were low and the grain size (p > 63 μm) was relatively stable, but there was a marked decrease of Poaceae and Fabaceae. These results suggest that abandonment of ancient cities, such as Loulan and Hami, peaked during the fourth and fifth centuries, possibly because of population reduction as a result of war.

Our results demonstrate that natural environment of the study area changed strongly during 1.3–1.0 kyr. During the seventh and eighth centuries, very high concentrations of micro charcoal were deposited, which then fell sharply to their lowest values in the eighth and ninth centuries (1.2–1.0 kyr). The increased sand content and relatively lower pollen concentration in the KLA record indicate that the climate in southern Xinjiang became more arid and the environment changed (Figures 3, 4, 5A, 6B,E). Because of human activities markedly increased, the ability of humans to influence the environment was reinforced, and so the environment changed more. From the second half of the seventh century onwards, several wars broke out between the Tibetan regime and the Tang ruler. As a result, the number of households in the Yutian region decreased from 32,000 in the Han Dynasty to 4,487 in the Tang Dynasty; thus, only one-seventh of the population was left (Zu et al., 2003). This information suggests that the war was one of the reasons for abandonment of ancient cities.

From the 13th to 17th centuries (the Yuan and Ming dynasties), the charcoal concentration was low. During this interval, the political situation was unstable and a persistent religious war broke out between the Kaxgar kalahan region and the Yutian-xizhou Huihu region. As a result, the religious reign over the western region came to an end and the region's flourishing economy was also destroyed (Zhong and Xiong, 1999; Zu et al., 2003). The climate was dry and cold during the Little Ice Age (Figure 6). In the United States and Europe, the charcoal abundance at this stage was the lowest since 2000 BP (Wang et al., 2010), as was also the case in the southern margin of the Tarim Basin.

To summarize, the paleoclimatic and archaeological data suggest a temporal correlation between aridity changes and human activity. Our results indicate that the abrupt changes of climate, intensified human activity and fire regime were the major drivers of the charcoal peak in the Kunlun highland and the Tarim Basin. We tentatively conclude that human activity, although not the sole reason, was an important explanation for the abandonment of ancient cities in the hyperarid Tarim.

6 Conclusion

We applied pollen and charcoal data from the sediments of the KLA loess section to reconstruct paleoclimate and paleoenvironmental changes and human activity in southern Xinjiang during the middle Holocene. The pollen record of the KLA section reveals a slightly drying trend with pronounced moisture fluctuations on the Kunlun highland during the past 4,900 years. Stronger human activities commenced at approximately 2.0 kyr. Macro and micro charcoal showed different temporal patterns during the middle Holocene, we propose that the micro charcoal originated in the Tarim Basin, reflecting human activity in the basin. Macro charcoal can be applied to infer Kunlun highland fire events. We suggest that human impacts on the natural mountain vegetation of the Kunlun highland commenced prior to ~4.9 kyr. Relatively stable and lower macro charcoal concentrations reflected human activities that were less affected by climate change. Our study provides a new and potentially important method for studying climatic change in inland arid areas of China during the middle Holocene. Further research on historic paleoclimatic and paleoenvironmental changes and human–land relationships in southern Xinjiang will assist in improving the accuracy of predictions of future climatic trends.

Data availability statement

The raw data supporting the conclusion of this article will be made available by the authors, without undue reservation.

Author contributions

Conceptualization, YP; methodology, GW; software,GM and CG; validation, DL; formal analysis, GW; writing—original draft preparation, YP; writing—review and editing, HB. All authors have read and agreed to the published version of the manuscript.

Funding

This work was supported by the National Natural Science Foundation of China (Grant Nos. 41601197 and 42105071), and project of science and technology of the Henan province for tackling key problems (No. 212102110390).

Conflict of interest

The authors declare that the research was conducted in the absence of any commercial or financial relationships that could be construed as a potential conflict of interest.

Publisher's note

All claims expressed in this article are solely those of the authors and do not necessarily represent those of their affiliated organizations, or those of the publisher, the editors and the reviewers. Any product that may be evaluated in this article, or claim that may be made by its manufacturer, is not guaranteed or endorsed by the publisher.

References

An, C., Feng, Z., and Barton, L. (2006). Dry or humid? Mid-holocene humidity changes in arid and semi-arid China. *Quat. Sci. Rev.* 25, 351–361. doi:10.1016/j.quascirev.2005.03.013

Blaauw, M. (2010). Methods and code for 'classical' age-modelling of radiocarbon sequences. *Quat. Geochronol.* 5 (5), 512–518. doi:10.1016/j.quageo.2010.01.002

Chen, F., Bo, C., Zhao, Y., Zhu, Y., and Madsen, D. B. (2006). Holocene environmental change inferred from a high-resolution pollen record, Lake Zhuyeze, arid China. *Holocene* 16, 675–684. doi:10.1191/0959683606hl951rp

Chen, F., Yu, Z., Yang, M., Ito, E., Wang, S., Madsen, D. B., et al. (2008). Holocene moisture evolution in arid central Asia and its out-of-phase relationship with Asian monsoon history. *Quat. Sci. Rev.* 27, 351–364. doi:10.1016/j.quascirev.2007.10.017

Chen, W., Meng, H., Song, H., and Zheng, H. (2022). Progress in dust modelling, global dust budgets, and soil organic carbon dynamics. *Land* 176, 1020176. doi:10.3390/land11020176

Chen, Z., Chen, Y., Li, W., and Chen, Y. (2011). Changes of runoff consumption and its human influence intensity in the mainstream of Tarim river. *Acta Geogr. Sin.* 66 (1), 89. doi:10.11821/xb201101009

Clark, J. S. (1988). Particle motion and the theory of charcoal analysis: Source area, transport, deposition, and sampling. *Quat. Res.* 30, 67–80. doi:10.1016/0033-5894(88)90088-9

Clark, J. S., and Patterson, W. A. (1997). "Background and local charcoal in sediments: Scales of fire evidence in the paleorecord," in *Sediment records of biomass burning and global change NATO ASI series*. Editors J. S. Clark, H. Cachier, J. G. Goldammer, and B. Stocks (Berlin: Springer), 51. doi:10.1007/978-3-642-59171-6_3

Cour, P., Zheng, Z., Duzer, D., Calleja, M., and Yao, Z. (1999). Vegetational and climatic significance of modern pollen rain in northwestern Tibet. *Rev. Palaeobot. Palynology* 104, 183–204. doi:10.1016/s0034-6667(98)00062-1

Cui, H., Wang, B., Qi, G., and Zhang, X. (1988). Vegetation types on northern slopes and the interior of central Kunlun Mountains. *Acta Phytoecol. Geobotanica Sinica* 12 (2), 91.

Dodson, J. R., Taylor, D., Ono, Y., and Wang, P. (2004). Climate, human, and natural systems of the PEP II transect. *Quat. Int.* 118–119, 3–12. doi:10.1016/s1040-6182(03)00127-7

Domrös, M., and Peng, G. (1988). *The climate of China*. Berlin: Springer.

Du, Z. (1996). Influence of the East-West difference of climatic changes since recent 2000 years on the rise and decline of the Silk Road in China. *Arid. Land Geogr.* 19 (3), 50.

El-Moslimany, A. P. (1990). Ecological significance of common nonarboreal pollen: Examples from drylands of the Middle East. *Rev. Palaeobot. Palynology* 64, 343–350. doi:10.1016/0034-6667(90)90150-h

Fægri, K., and Iversen, J. (1989). *Textbook of pollen analysis*. New York: Publisher John Wiley and Sons.

Fang, X., Lü, L., Yang, S., Li, J., An, Z., Jiang, P., et al. (2002). Loess in Kunlun Mountains and its implications on desert development and Tibetan Plateau uplift in west China. *Sci. China Ser. D-Earth. Sci.* 45, 289–299. doi:10.1360/02yd9031

Finsinger, W., Tinner, W., and Hu, F. (2008). "Rapid and accurate estimates of microcharcoal content in pollen slides," in *Charcoals from the past: Cultural and paleoenvironmental implications: Proceedings of the third international meeting of anthracology, cavallino-lecce (Italy) 2004*. Editors G. Fiorentino and D. Magri (Oxford: Hadrian Press), 121–124.

Gao, C. (2004). Sedimentary facies changes and climatic-tectonic controls in a foreland basin, the Urumqi River, Tian Shan, Northwest China. *Sediment. Geol.* 169, 29–46. doi:10.1016/j.sedgeo.2004.04.006

Gao, C., and Zhang, Q. (1991). Preliminary study on loess and its sedimentary conditions on northern slopes of Kunlun Mountains. *Geogr. Res.* 10 (4), 40.

Goldberg, E. (1985). *Black carbon in the environment*. New York: Publisher John Wiley and Sons.

Goudie, A. (2002). *Great warm deserts of the world: Landscapes and evolution*. Oxford: Oxford University Press.

Han, Y., Yang, S., Fang, X., and Song, L. (2006). Atmospheric circulation in Tarim Basin and loess accumulation in northern slopes of Kunlun Mountains. *J. Desert Res.* 26, 351

Hovermann, J., and Hovermann, E. (1991). Pleistocene and Holocene geomorphological features between the Kunlun mountains and the Taklimakan Desert. *Die Erde* 6, 51.

Huang, C. C., Pang, J., Chen, S., Su, H., Han, J., Cao, Y., et al. (2006). Charcoal records of fire history in the Holocene loess–soil sequences over the southern Loess Plateau of China. *Palaeogeogr. Palaeoclimatol. Palaeoecol.* 239, 28–44. doi:10.1016/j.palaeo.2006.01.004

Huang, W. (1981). *History and geography of northwest China*. Shanghai: Shanghai People's Publication House, 223.

Huang, X., Chen, C., Jia, W., An, C., Zhou, A., Zhang, J., et al. (2015). Vegetation and climate history reconstructed from an alpine lake in central tienshan mountains since 8.5 ka BP. *Palaeogeogr. Palaeoclimatol. Palaeoecol.* 432, 36–48. doi:10.1016/j.palaeo.2015.04.027

Huang, X., Xiang, L., Lei, G., Sun, M., Qiu, M., Storozum, M., et al. (2021). Sedimentary pediastrum record of middle–late holocene temperature change and its impacts on early human culture in the desert-oasis area of northwestern China. *Quat. Sci. Rev.* 265, 107054. doi:10.1016/j.quascirev.2021.107054

Huang, X., Zhang, J., Storozum, M., Liu, S., Gill, J. L., Xiang, L., et al. (2020). Long-term herbivore population dynamics in the northeastern Qinghai-tibetan Plateau and its implications for early human impacts. *Rev. Palaeobot. Palynology* 275, 104171. doi:10.1016/j.revpalbo.2020.104171

Hui, Z., Gowan, E. J., Hou, Z., Zhou, X., Ma, Y., Guo, Z., et al. (2021). Intensified fire activity induced by aridification facilitated Late Miocene C4 plant expansion in the northeastern Tibetan Plateau, China. *Palaeogeogr. Palaeoclimatol. Palaeoecol.* 573, 110437. doi:10.1016/j.palaeo.2021.110437

Jakel, D. (1991). The evolution of dune fields in the Taklimakan Desert since the Late Pleistocene, Notes on the 1:2, 500, 000 map of dune evolution in the Takamakan. *Die Erde* 6, 191.

Jiao, D., Xie, S., Yang, H., Xiang, S., and Wang, X. (2009). Paleofire indicated by triterpenes and charcoal in a culture bed in eastern Kunlun Mountain, Northwest China. *Front. Earth Sci. China* 3, 452–456. doi:10.1007/s11707-009-0053-1

Li, B., Dong, G., Zhu, Y., Li, S., Ren, X., Jin, H., et al. (1993). Desert and loess in tarim basin and their depositional conditions since the last glaciation. *Sci. China* 23, 644.

Li, J, J. (1985). "The relationship between climatic change and disappearance of the old Loulan Country and the change of the Old Silk Road," in *Contributions to quaternary environments of arid Xinjiang* (Urmuqi: University of XinjiangXinjiang People's Publishing House), 81.

Li, Y, Y. (1985). Evolution of desert and oasis in hotan region. *J. Xinjiang Univ. Soc. Part)* 3, 70.

Liu, D. (1988). "Population problems in hotan region," in *Study on hotan oasis*. Editor H. Chen (Urumqi: Xinjiang People's Publishing House), 162.

Liu, T. (1965). *Loess deposits in China (in Chinese)*. Beijing: China Ocean Press.

Liu, X., Zhong, Y., Wang, M., He, Q., Maimaitimin, A., and Bai, L. (2010). Atmospheric dustfall variation and factor analysis in Tarim Basin. *J. Desert Res.* 30, 954.

Luo, C., Zheng, Z., Tarasov, P., Pan, A., Huang, K., Beaudouin, C., et al. (2009). Characteristics of the modern pollen distribution and their relationship to vegetation in the xinjiang region, northwestern China. *Rev. Palaeobot. Palynology* 153, 282–295. doi:10.1016/j.revpalbo.2008.08.007

Marsicek, J., Shuman, B. N., Bartlein, P. J., Shafer, S. L., and Brewer, S. (2018). Reconciling divergent trends and millennial variations in Holocene temperatures. *Nature* 554, 92–96. doi:10.1038/nature25464

Patterson, W. A., Edwards, K. J., and Maguire, D. J. (1987). Microscopic charcoal as a fossil indicator of fire. *Quat. Sci. Rev.* 6, 3–23. doi:10.1016/0277-3791(87)90012-6

R Development Core Team (2010). *R: A language and environment for statistical computing*. Vienna: R Foundation for Statistical Computing. Available at: http://www.R-project.org.

Ramsey, C. B. (2008). Deposition models for chronological records. *Quat. Sci. Rev.* 27, 42–60. doi:10.1016/j.quascirev.2007.01.019

Ramsey, C. B., and Lee, S. (2013). Recent and planned developments of the program OxCal. *Radiocarbon* 55 (2), 720–730. doi:10.1017/S0033822200057878

Rao, Z., Huang, C., Xie, L., Shi, F., Zhao, Y., Cao, J., et al. (2019). Long-term summer warming trend during the Holocene in central Asia indicated by alpine peat α-cellulose δ13C record. *Quat. Sci. Rev.* 203, 56–67. doi:10.1016/j.quascirev.2018.11.010

Reimer, P. J., Austin, W. E. N., Bard, E., Bayliss, A., Blackwell, P. G., Ramsey, C. B., et al. (2020). The IntCal20 northern hemisphere radiocarbon age calibration curve (0–55 cal kBP). *Radiocarbon* 62, 725–757. doi:10.1017/RDC.2020.41

Rhodes, A. N. (1998). A method for the preparation and quantification of microscopic charcoal from terrestrial and lacustrine sediment cores. *Holocene* 8, 113–117. doi:10.1191/095968398671104653

Sadori, L., and Giardini, M. (2007). Charcoal analysis, a method to study vegetation and climate of the Holocene: The case of Lago di Pergusa (Sicily, Italy). *Geobios* 40, 173–180. doi:10.1016/j.geobios.2006.04.002

Scott, A. C., Moore, J., and Brayshay, B. (2000). Introduction to fire and the palaeoenvironment. *Palaeogeogr. Palaeoclimatol. Palaeoecol.* 164, 7. doi:10.1016/S0031-0182(00)00165-6

Shu, Q., Zhong, W., and Li, C. (2007). Distribution feature of ancient ruins in south edge of tarim basin and relationship with environmental changes and human activities. *J. Arid Land Resour. Environ.* 21 (11), 95.

Shu, Q., Zhong, W., and Xiong, H. (2003). Study on the paleoclimatic evolution and the vicissitude of human being's civilization in Tarim Basin since about 4.0k years. *Hum. Geogr.* 18 (3), 87. doi:10.13959/j.issn.1003-2398.2003.03.019

Stevenson, J., and Haberle, S. (2005). *Macro charcoal analysis: A modified technique used by the department of Archaeology and natural history*. Canberra, Australia: Australian National University.

Sun, J. (2002). Source regions and formation of the loess sediments on the high mountain regions of northwestern China. *Quat. Res.* 58, 341–351. doi:10.1006/qres.2002.2381

Tan, Z., Huang, C. C., Pang, J., and Zhou, Q. (2011). Holocene wildfires related to climate and land-use change over the weihe river basin, China. *Quat. Int.* 234, 167–173. doi:10.1016/j.quaint.2010.03.008

Tang, Z., Chen, D., Wu, X., and Mu, G. (2013). Redistribution of prehistoric tarim people in response to climate change. *Quat. Int.* 308-309, 36–41. doi:10.1016/j.quaint.2013.01.021

Tang, Z., Mu, G., and Chen, D. (2009). Palaeoenvironment of mid- to late holocene loess deposit of the southern margin of the tarim basin, NW China. *Environ. Geol.* 58, 1703–1711. doi:10.1007/s00254-008-1670-9

Thevenon, F., Williamson, D., Bard, E., Anselmetti, F. S., Beaufort, L., and Cachier, H. (2010). Combining charcoal and elemental black carbon analysis in sedimentary archives: Implications for past fire regimes, the pyrogenic carbon cycle, and the human–climate interactions. *Glob. Planet. Change* 72 (4), 381–389. doi:10.1016/j.gloplacha.2010.01.014

Thompson, L. G., Yao, T., Davis, M. E., Henderson, K. A., Mosley-Thompson, E., Lin, P., et al. (1997). Tropical climate instability: The last glacial cycle from a qinghai-Tibetan ice core. *Science* 276 (5320), 1821–1825. doi:10.1126/science.276.5320.1821

Wagner, M., Wu, X., Tarasov, P., Aisha, A., Ramsey, C. B., Schultz, M., et al. (2011). Radiocarbon-dated archaeological record of early first millennium B.C. mounted pastoralists in the Kunlun Mountains, China. *Proc. Natl. Acad. Sci. U. S. A.* 108 (38), 15733–15738. doi:10.1073/pnas.1105273108

Wang, Z., Chappellaz, J., Park, K., and Mak, J. E. (2010). Large variations in southern hemisphere biomass burning during the last 650 years. *Science* 330 (6011), 1663–1666. doi:10.1126/science.1197257

Whitlock, C., and Larsen, C. (2001). "Charcoal as a fire proxy," in *Tracking environmental change using lake sediments*. Editors J. P. Smol, H. J. B. Birks, W. M. Last, R. S. Bradley, and K. Alverson (Berlin: Developments in Paleoenvironmental ResearchSpringer), 3, 75–98. doi:10.1007/0-306-47668-1_5

Xi, J. (1988). "Oasis distribution at south part of tarim basin in history period," in *Natural Resources Research Association of ChinaStudy on natural resources of the arid and semi-arid regions in China* (Beijing: Science Press), 132.

Xinjiang Archaeological Team, IA, CASS (2016). Liushui cemetery of the bronze age in yutian county, Xinjiang. *Archaeology* 12, 19–36. [in Chinese].

Yang, X., Du, J., Liang, P., Zhang, D., Chen, B., Rioual, P., et al. (2021). Palaeoenvironmental changes in the central part of the taklamakan desert, northwestern china since the late Pleistocene. *Chin. Sci. Bull.* 66 (24), 3205–3218. (in Chinese). doi:10.1360/tb-2020-1383

Yang, X. (1991). "Geomorphologische Untersuchungen in den Trockenräumen NW-Chinas unter besonderer Berücksichtigung von Badanjilin und Takelamagan," in *Göttinger geographische abhandlungen* (Göttingen: Verlag Erich Goltze).

Yang, X., Rost, K. T., Lehmkuhl, F., Zhu, Z., and Dodson, J. (2004). The evolution of dry lands in northern china and in the republic of mongolia since the last glacial maximum. *Quat. Int.* 118–119, 69–85. doi:10.1016/s1040-6182(03)00131-9

Yang, X., Zhu, Z., Jaekel, D., Owen, L. A., and Han, J. (2002). Late quaternary palaeoenvironment change and landscape evolution along the keriya river, Xinjiang, China: The relationship between high mountain glaciation and landscape evolution in foreland desert regions. *Quat. Int.* 97 (98), 155–166. doi:10.1016/s1040-6182(02)00061-7

Yao, T., Thompson, L. G., Qin, D., Tian, L., Jiao, K., Yang, Z., et al. (1996). Variations in temperature and precipitation in the past 2000 a on the xizang (Tibet) plateau-guliya ice core record. *Sci. China Ser. D Earth Sci.* 39, 425.

Zan, J., Fang, X., Yang, S., Nie, J., and Li, X. (2010). A rock magnetic study of loess from the west kunlun mountains. *J. Geophys. Res.* 115, B10101. doi:10.1029/2009jb007184

Zhao, X., Maimaiti, Y., Liu, J., Luo, J., and Ruan, C. (1995). Depositional characteristics and environmental evolution of loess in keriya river basin since late pleistocene. *Arid. Land Geogr.* 18 (1), 52.

Zhao, Y., Yu, Z., Chen, F., Ito, E., and Zhao, C. (2007). Holocene vegetation and climate history at hurleg lake in the qaidam basin, northwest China. *Rev. Palaeobot. Palynology* 145, 275–288. doi:10.1016/j.revpalbo.2006.12.002

Zheng, H., Ren, Q., Zheng, K., Qin, Z., Wang, Y., and Wang, Y. (2022). Spatial distribution and risk assessment of metal(loid)s in marine sediments in the arctic ocean and bering Sea. *Mar. Pollut. Bull.* 179, 113729. doi:10.1016/j.marpolbul.2022.113729

Zhong, W., Wang, L., Xiong, H., and Nuerbai (2007). Climate-environment changes and possible human activity effect since mid-holocene in hetian oasis, southern margin of Tarim basin. *J. Desert Res.* 27 (2), 171.

Zhong, W., and Xiong, H. (1999). Paleo-climatic and environmental development since about 4 ka BP and the relation with abandonments of ancient cities in Southern Xinjiang. *J. Desert Res.* 19 (4), 343.

Zhong, W., Xiong, H., Tash, P., Hiroki, T., and Shu, Q. (2001). Paleoclimatic and paleoenvironmental changes in southern Xinjiang during historical period. *Acta Geogr. Sin.* 56 (3), 345. doi:10.11821/xb200103011

Zhou, Y., Yang, X., Zhang, D., Mackenzie, L. L., and Chen, B. (2021). Sedimentological and geochemical characteristics of sediments and their potential correlations to the processes of desertification along the keriya river in the taklamakan desert, Western China. *Geomorphology* 375, 107560. doi:10.1016/j.geomorph.2020.107560

Zhu, Z., Chen, Z., Wu, Z., Li, J., Li, B., and Wu, G. (1981). *Study on the Geomorphology of wind-drift sands in the taklamakan desert*. Beijing: Science Press.

Zhu, Z., and Lu, J. (1991). A study on the formation and development of aeolian landforms and the trend of environmental changes in the lower reaches of the Keriya River, Central Taklimakan Desert. *Die Erde* 6, 89.

Zu, R., Gao, Q., Qu, J., and Qiang, M. (2003). Environmental changes of oases at southern margin of Tarim Basin, China. *Environ. Geol.* 44, 639–644. doi:10.1007/s00254-003-0808-z